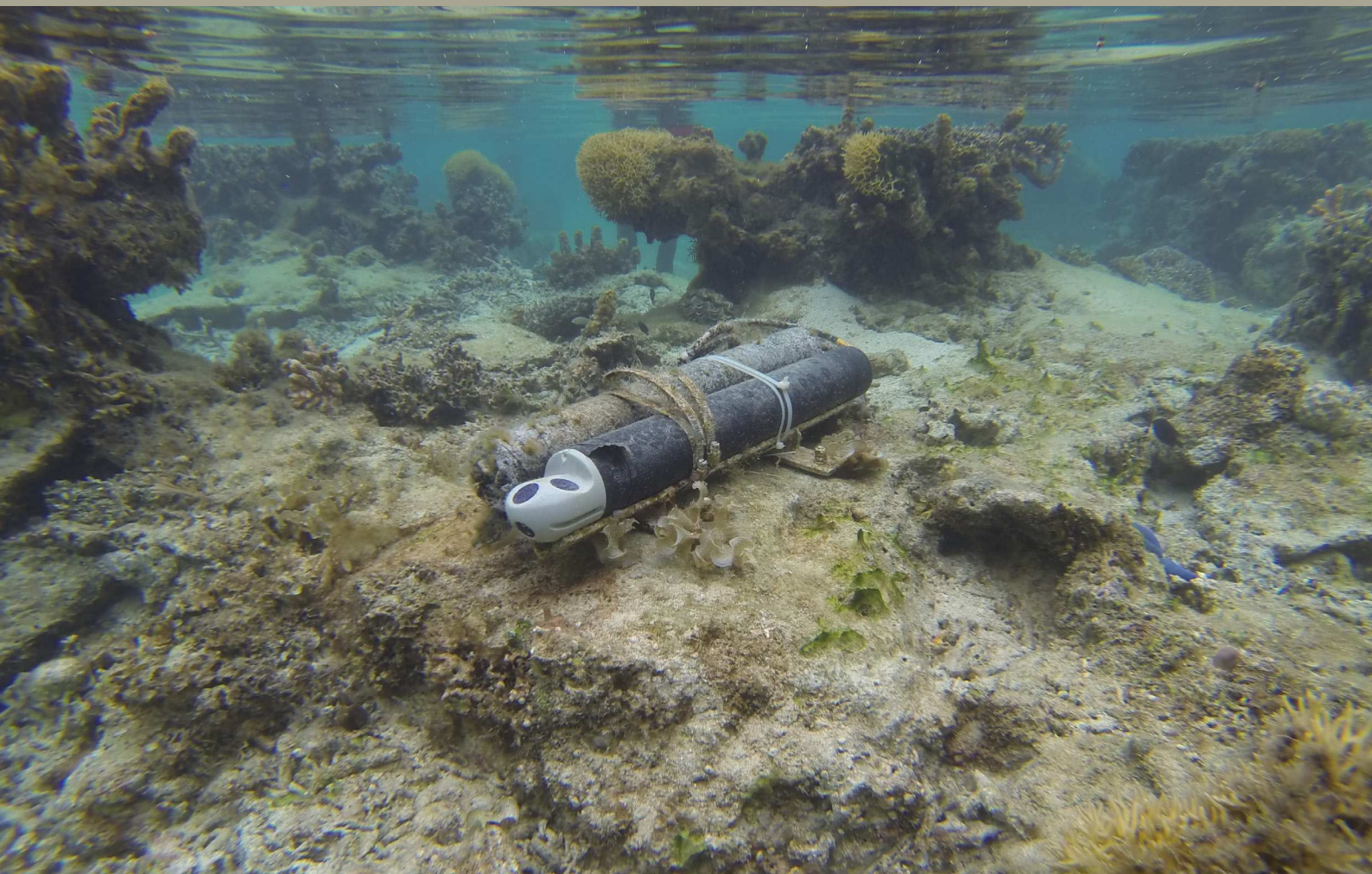


# Waves and Coasts in the Pacific

Maui Bay (Fiji), Oceanographic  
Data Collection



Cyprien Bosserelle, Deepika Lal, Sandeep Reddy,  
Make Movono, Zulfikar Begg, Salesh Kumar, Jens Krüger



Pacific  
Community  
Communauté  
du Pacifique



UNESCO-IHE  
Institute for Water Education





# Waves and Coasts in the Pacific (WACOP)

Maui Bay (Fiji), Oceanographic data collection

Cyprien Bosserelle, Deepika Lal, Sandeep Reddy, Make Movono,  
Zulfikar Begg, Salesh Kumar, Jens Krüger



[www.gsd.spc.int/wacop/](http://www.gsd.spc.int/wacop/)

© Pacific Community (SPC) 2016

All rights for commercial / for profit reproduction or translation, in any form, reserved. SPC authorises the partial reproduction or translation of this material for scientific, educational or research purposes, provided that SPC and the source document are properly acknowledged. Permission to reproduce the document and/or translate in whole, in any form, whether for commercial / for profit or non-profit purposes, must be requested in writing. Original SPC artwork may not be altered or separately published without permission.

Original text: English

SPC technical Report SPC00036

May 2016

This research was conducted as part of the Waves and Coasts in the Pacific project (WACOP project), financed by the European Union, Grant Number FED/2011/281-131.

**DISCLAIMER**

While care has been taken in the collection, analysis, and compilation of the data, they are supplied on the condition that the Pacific Community shall not be liable for any loss or injury whatsoever arising from the use of the data.

The contents of this publication are the sole responsibility of the Pacific Community and can in no way be taken to reflect the views of the European Union or other partners of the WACOP project.

Pacific Community  
Geoscience Division (GSD)  
Private Mail Bag, GPO Suva, Fiji Islands  
Telephone: (679) 338 1377  
Fax: (679) 337 0040  
Email: [cyprienb@spc.int](mailto:cyprienb@spc.int)  
[www.spc.int](http://www.spc.int)  
[www.gsd.spc.int/wacop/](http://www.gsd.spc.int/wacop/)

## Contents

<b>Acknowledgements</b> .....	5
<b>Executive summary</b> .....	6
1 Background .....	7
1.1 Aims of the WACOP project .....	7
1.2 This report.....	7
2 Site Overview .....	8
2.1 Morphology.....	8
3 Method .....	10
3.1 Deployments.....	10
3.2 Oceanographic data Post processing.....	14
3.2.1 Waves.....	14
3.2.2 Water levels .....	15
3.2.3 Currents.....	15
3.2.4 Tide.....	15
4 Results.....	16
4.1 Waves.....	16
4.1.1 Reef slope.....	16
4.1.2 Reef crest .....	17
4.1.3 Mid-reef .....	19
4.1.4 Shore .....	21
4.2 Water level.....	22
4.2.1 Reef slope.....	22
4.2.2 Reef crest .....	23
4.2.3 Mid Reef.....	23
4.2.4 Shore .....	24
4.3 Temperature .....	24
4.3.1 Reef slope.....	24
4.3.2 Reef crest .....	25
4.3.3 Mid Reef.....	25
4.3.4 Shore .....	26
4.4 Tides.....	26
4.4.1 Exceedance Curve .....	27

4.5	Currents.....	28
5	Discussion.....	28
5.1	Tide and wave setup in the reef flat .....	29
5.2	Infragravity waves.....	30
6	Conclusion.....	31
7	Data download and Citation .....	31
8	Reference .....	32

## Acknowledgements

This work is part of the Waves and Coasts in the Pacific (WACOP) project, which is implemented by the Pacific Community (SPC) in collaboration with the University of the South Pacific, UNESCO-IHE, the Commonwealth Scientific and Industrial Research Organisation (CSIRO), and the University of Auckland. This project was funded under the ACP Caribbean & Pacific Research Programme for Sustainable Development, a programme funded by the European Union (EU) and implemented by the African, Caribbean and Pacific Group of States (ACP Group).

The data presented in this study has been collected with the support and approval of the Fiji government and the Coral Coast communities of Tagaqe and Votua. Many staff of the Pacific Community, the University of the South Pacific and the University of Auckland and the Mineral Resource Department of Fiji were actively involved in the field data collection and in particular, Isei Rayawa, Eddie Beetham, Paul Kench, Susan Pohler, Aseri Baleilevuka.

The authors would like to thank the Maui Bay Community and Julian Hennings for their support towards the project and for making their boat available, also Epli for driving the boat during surveys and for having a sharp eye to help find instruments for recovery.

## **Executive summary**

Understanding the wave climate changes in the Pacific region is critical for coastal management and to the implementation of climate change adaptation. However, little is known about waves and how reef hydrodynamics is affecting the reef coast of Pacific islands. The Changing Waves and Coast in the Pacific (WACOP) project is collecting baseline information and using the latest research tools to assess the wave climate, its variability, improve the understanding of reef hydrodynamics and morphology as well as predict how these will change with the climate. The project aim is to better understand coastal erosion and inundations and to assess the potential for wave energy harvesting.

The data presented in this document analyses the oceanographic data record. The data shows how waves transform and dissipate as they cross the reef flat fronting Maui Bay on the Coral Coast. The data also shows that infragravity waves dominate the reef flat hydrodynamics. The data also shows evidence of seasonal internal waves on the reef crest that may be playing an important role in bringing nutrient to the coral communities on reef slope.

The data presented here is the baseline of a more in-depth analysis of the hydrodynamics of Maui Bay (Bosslerelle et al. 2015) and is being used for further findings on reef hydrodynamics.



# 1 Background

The Pacific island countries (PICs) are vulnerable to climate change, and have a high dependence on imported fossil fuels. Both of these problems can be attributed to the smallness and geographic isolation of PICs. In terms of climate change, a specific disadvantage that arises from the smallness of the islands is a greater coastline to land-area ratio. The majority of urban areas are located in dynamic coastal zones, and, with a total population of 10 million, these tend to be densely populated with a relatively high concentration of infrastructure. The shorelines of PICs are therefore vulnerable areas with the greatest risk of displacement and loss of livelihood assets through erosion and inundation.

These coastal hazards are projected to become more frequent and intense with climate change. However, current coastal vulnerability and adaptation assessments still focus mainly on sea-level rise, with less attention paid to other important coastal change drivers such as ocean surface waves. Waves wear away land and remove beach sediments, and are also a cause of coastal flooding and habitat destruction during extreme events. Wave research is very limited in the PICs, particularly given their dependence on the coast. The limiting factor in assessing the effects of climate change on coastal areas is therefore insufficient information on the variability and trends of ocean waves as a driver of shoreline changes at relevant island and community scales.

PICs lag behind in research about wave climate variability and trends. Only a few short-term (years) *in-situ* wave observations exist, and there have only been a limited number of studies that analyse historical wave climate data in terms of coastal impacts and wave power availability. PICs do not currently conduct research into how wave climate, wave power, and shorelines may evolve under emissions scenarios. The poor understanding on how damaging waves, eroding shorelines and wave power have changed in the recent past and may change in the future under climate change is a major knowledge gap which will be addressed by the WACOP project.

## 1.1 Aims of the WACOP project

The project addressed these knowledge gaps in two ways. Firstly, in terms of ocean waves, the project used computer models to downscale public domain data on the historical (decadal) wave variability and trends to relevant regional and local scales, and estimate how wave climate will change in the future under projected climate change scenarios. Secondly, in terms of coastal inundation, field visits were conducted and data collected at specific local sites to calibrate and validate models (at scales of 10s of metres) that can predict inundation hazard under climate change and thereby assist with adaptation and disaster risk reduction. The majority of PIC coasts however are fringed by coral reefs, and adapting existing predictive models to reef environments will involve relevant and original research through this project.

## 1.2 This report

The field investigations presented in this report were aimed at gathering baseline information on the oceanography of the fringing reef and the beach fronting the shoreline in Maui Bay, on the Coral Coast of Fiji. This information is critical to better understand the role of waves in coastal hazards (erosion and inundation) in the Pacific. The Maui Bay site is one of 2 sites selected as the Project field sites. A similar report has been produced for the ocean side of Fatato Island on the atoll of Funafuti, in Tuvalu (Figure 1).

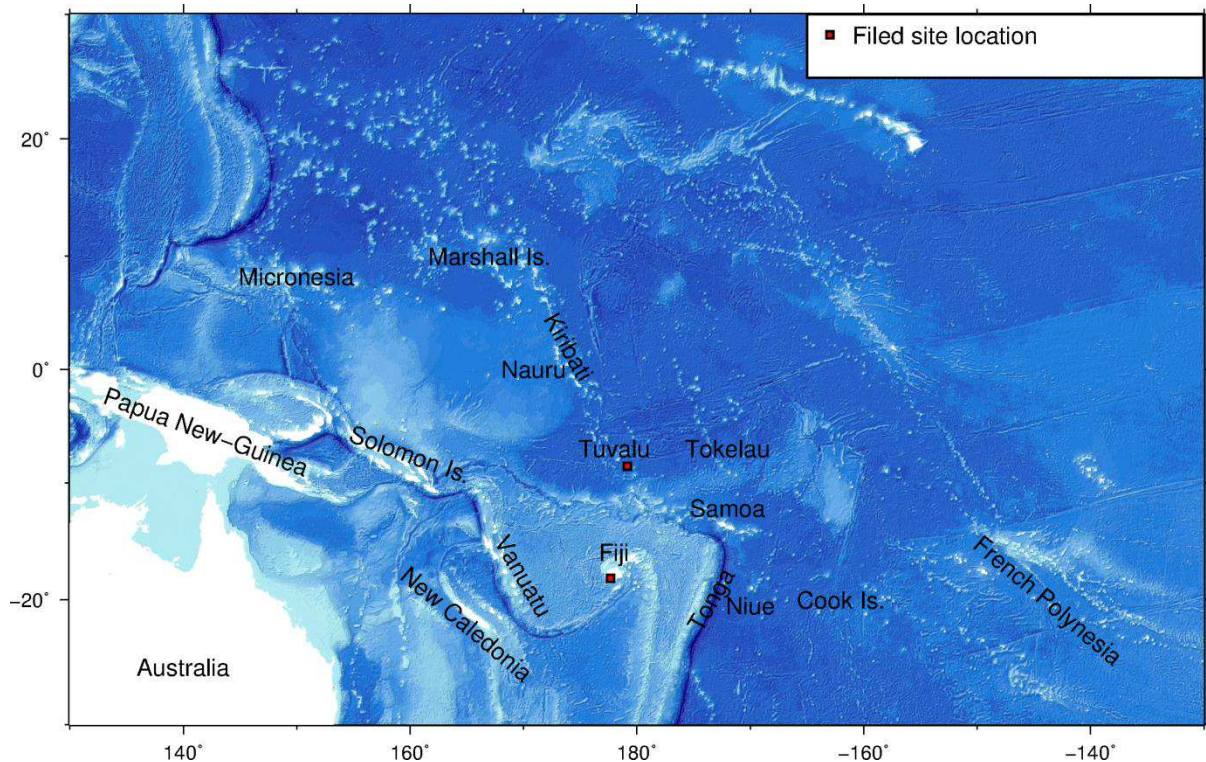


Figure 1.1 WACOP field sites in the Pacific

## 2 Site Overview

The Coral Coast is an area south of Viti Levu with a fringing reef system 400 – 800m wide interrupted by narrow passages. Maui Bay is the name of a development area located between the village of Tagaqe to the West and Votua-o-lailai to the East. The field site (Figure 2) corresponds to a 1,600m long shoreline from the Maui Bay jetty in the East to the Tagaqe passage in the West.

### 2.1 Morphology

Maui Bay field site is fronted by a fringing reef approx. 650m wide. The reef is bounded by a narrow passage (40m wide) to the east and the much wider Tagage passage (150m) to the west. The lagoon area of the fringing reef is relatively shallow (less than 1.5m deep) and is bounded east and west by a shallow algal ridge effectively forming a closed basin covering an area of 1.4km<sup>2</sup>.

The interior of the Lagoon is covered with an alternation between coral patches reaching close to mean sea level in elevation and sandy patch. Seagrass is present in the area but not extensively. The coral patches tend to be more common towards the reef crest and less towards the shore. 900m of the shoreline (Most of it on the East side) is fronted by a beachrock structure.

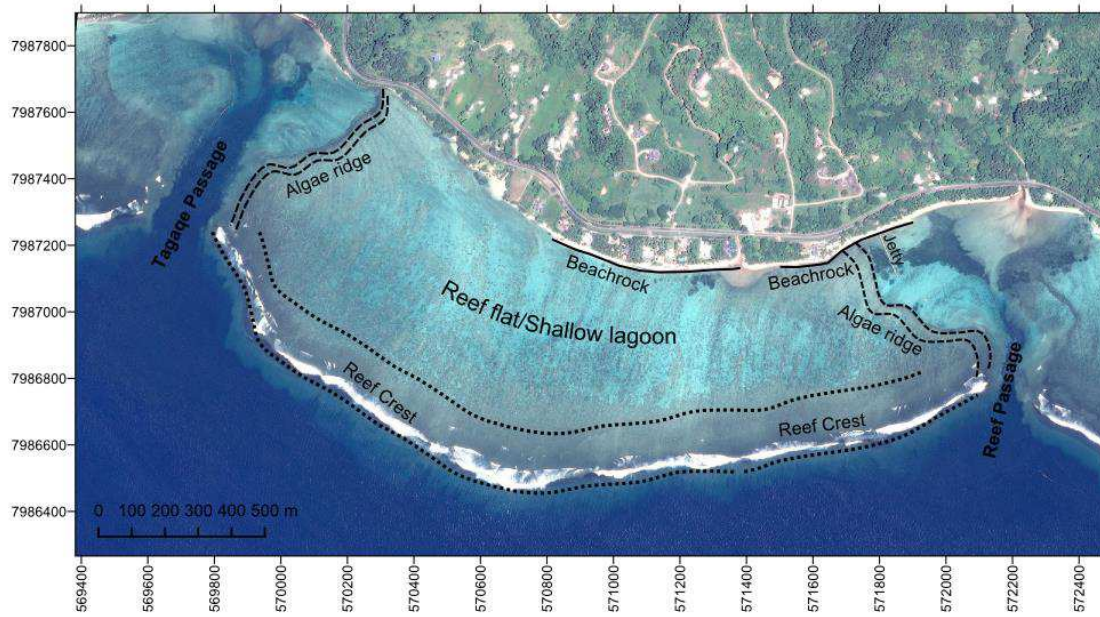


Figure 2.1. Location of beachrock and algae ridge in Maui Bay.

### 3 Method

A series of instruments were deployed in Maui Bay between January 2013 and November 2014 with the aim of measuring the local waves, currents, water level and water temperature across the reef from the offshore reef slope to the shore.

#### 3.1 Deployments

In Maui Bay, four oceanographic instruments were deployed along a cross-shore profile (Figure 3.1 and 3.2). A RBR-TWR pressure sensor was installed near the shore (Figure 3.3), an Aquadopp current profiler was installed in the centre of the lagoon (Figure 3.4), a RBR-TWR pressure sensor was installed near the reef crest (Figure 3.5) and a RDI-Workhorse current profiler was installed in the reef slope at approximately 20m depth, which later replaced by a AWAC current profiler. The brand and set up of each instrument is detailed in table 3.1. At the shore, mid reef and reef crest location, the reef was drilled and a temporary aluminium frame was bolted to the reef. This allowed for a consistent position of the instrument across multiple deployments and a secure mooring. The reef slope instrument was installed on the reef using a weighted aluminium frame. The frame was deployed and recovered with the instrument and redeployed at the same location each time.

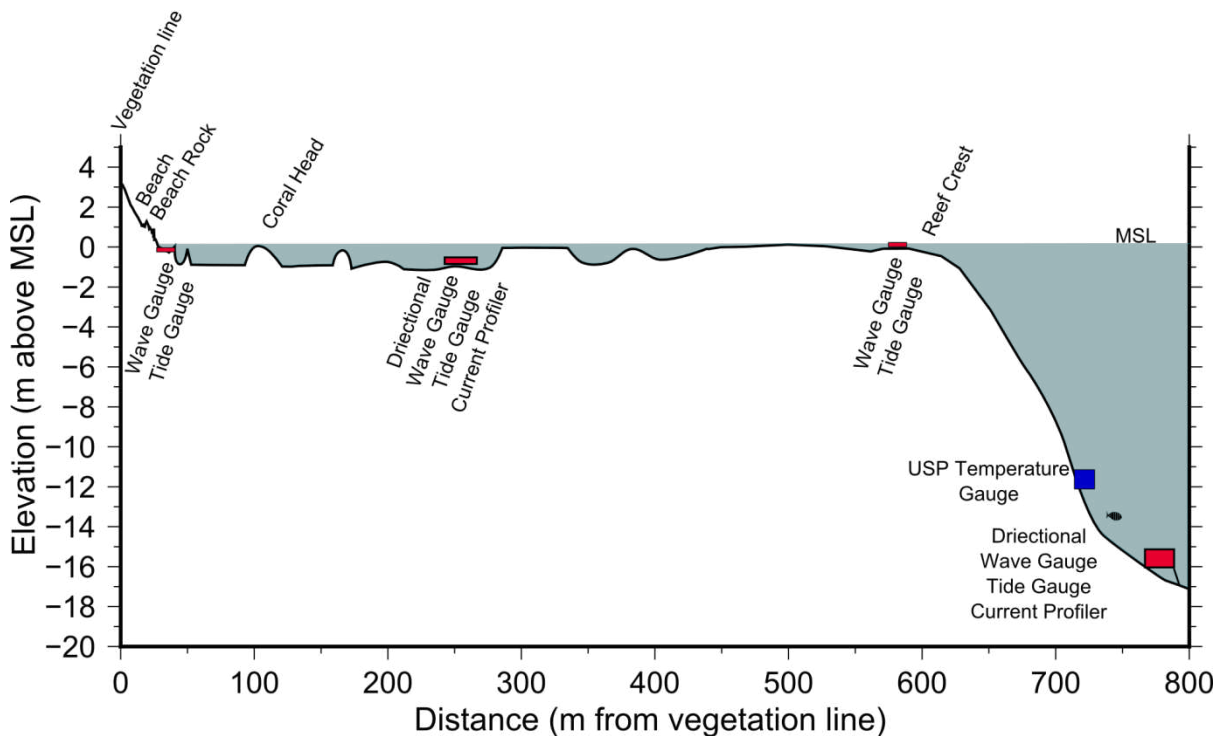


Figure 3.1. Bathymetric profile of Maui Bay showing the locations of oceanographic instruments.

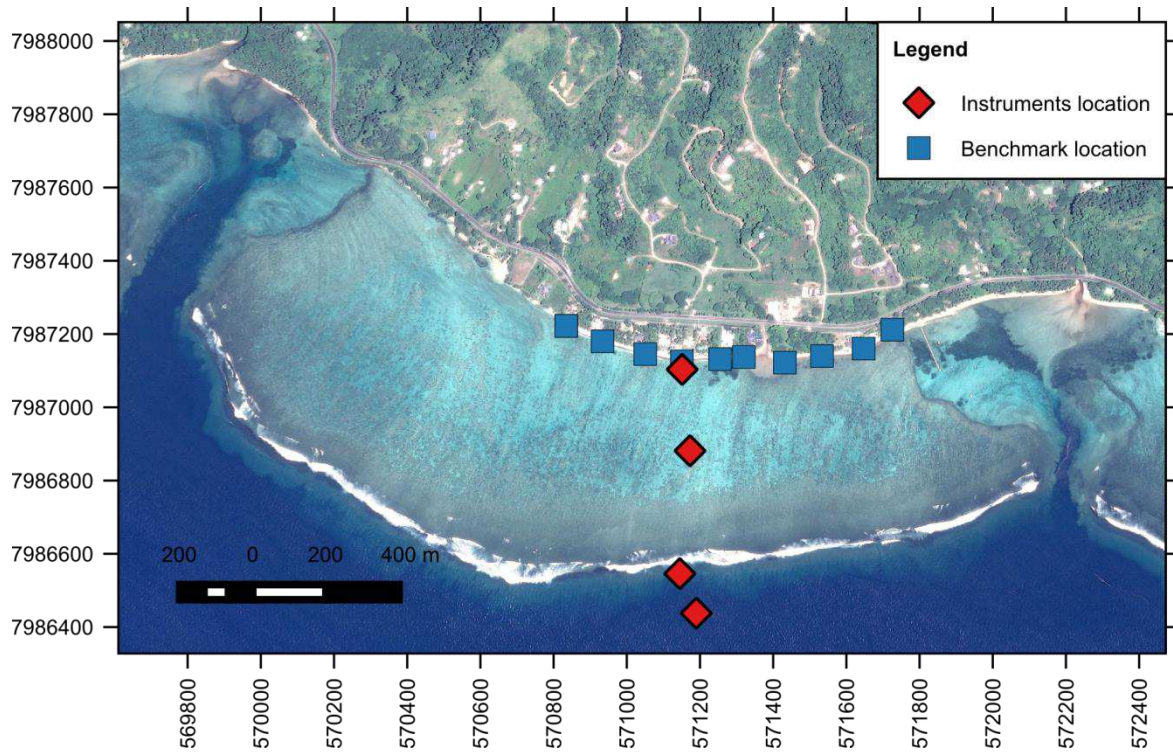


Figure 3.2 Maui Bay area; locations of instruments and Benchmarks.

Table 3.1 Instruments location

Name	Longitude	Latitude	Easting UTM60	Northing UTM60	Depth (m MSL)
Shore	177.6729	-18.2041	571,151.1	7,987,103.3	-0.29
Mid-Reef	177.6731	-18.2061	571,172.6	7,986,881.2	-0.37
Crest	177.6728	-18.2091	571,144.7	7,986,545.7	-0.40
Slope	177.6733	-18.2101	571,189.5	7,986,437.8	20.55

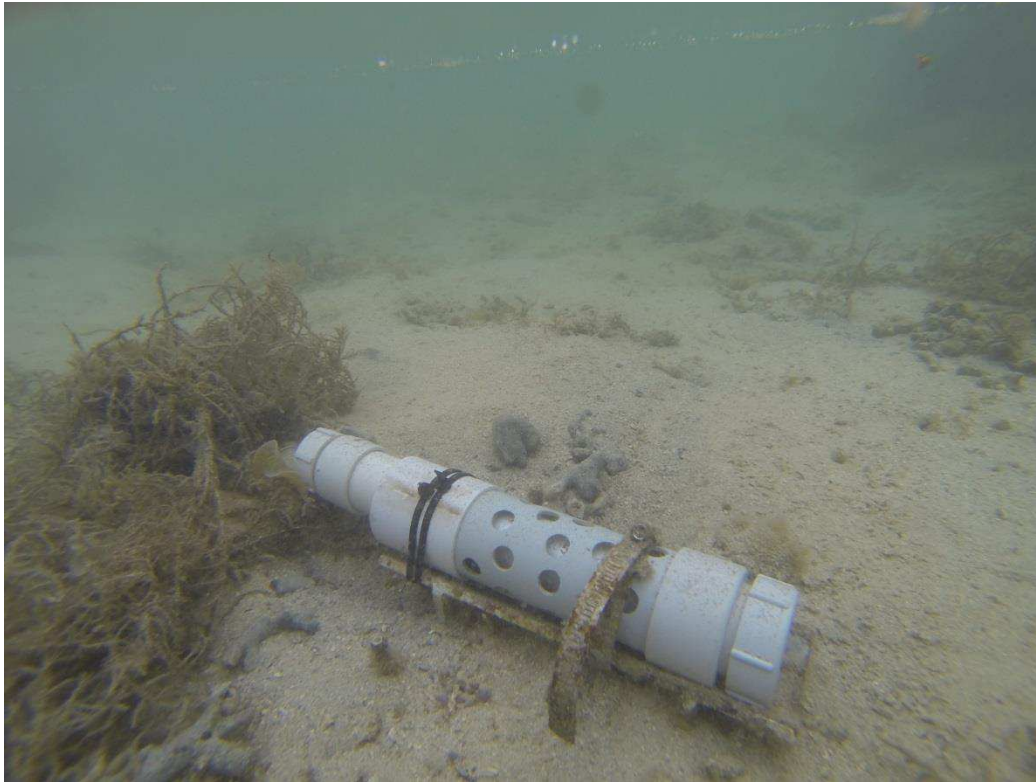


Figure 3.3 RBR-TWR deployed near the shore in Maui Bay



Figure 3.4 Aquadopp deployed near the centre of the reef flat in Maui Bay



Figure 3.5 RBR-TWR deployed near the reef crest in Maui Bay



Figure 3.6 RDI-Workhorse (University of Auckland) deployed on the reef slope of Maui Bay in 20m depth

Table 3.2

Brand - Instruments name	Location	Time between wave burst (s)	Wave burst duration (s)	Water level /currents ensemble averaging (s)	Interval between water level/currents ensembles (s)
RBR-TWR	Shore	10800	2048	240	600
Nortek - Aquadopp	Mid-reef	10800	2048	120	600
RBR-TWR	Reef Crest	10800	2048	240	600
RDI- Sentinel	Reef slope	10800	2048	120	1200
Nortek - AWAC	Reef slope	10800	2048	60	600

The deployment schedule used was designed to optimise the length of deployment hence instruments were swapped to limit data gaps between deployments. Some data gaps are unavoidable when instruments break down or batteries die out. A detail of the final schedule is presented in figure 3.7.

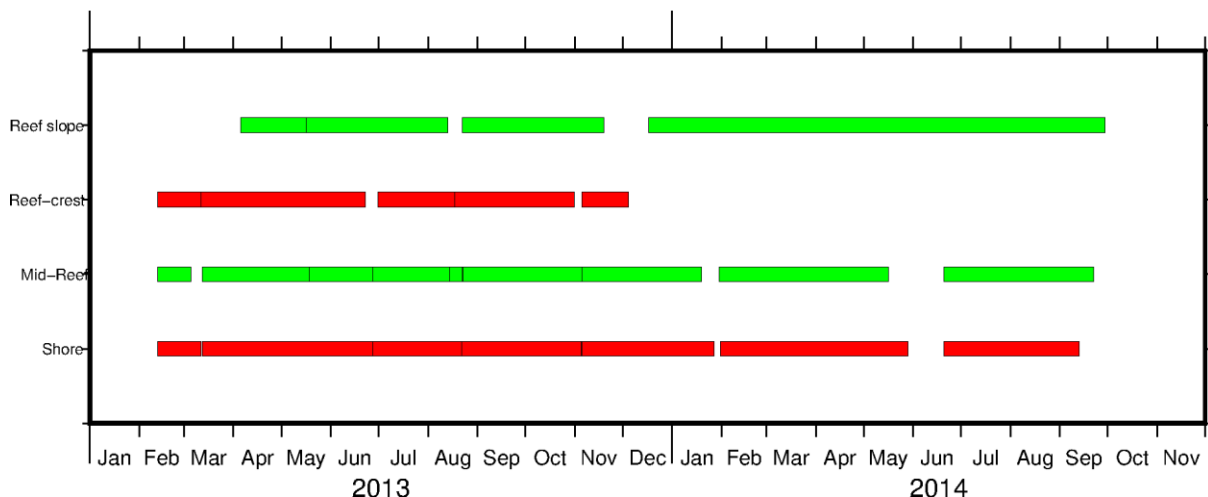


Figure 3.7 Oceanographic deployment schedules for each location in Maui Bay. This figure shows only the usable collected data. Note that on the reef crest, two consecutive instrument failures have prevented the collection of usable data in 2014.

### 3.2 Oceanographic data Post processing

The collected data was processed in a consistent way to allow comparison between locations.

#### 3.2.1 Waves

All wave data was collected in burst of pressure data at 1Hz. This data was processed by calculating the power spectrum of the detrended pressure measurements for each data burst using a one-side periodogram. For offshore sites each data burst was corrected to account for pressure damping due to the depth of the instrument. Based on the power spectrum of each burst, the significant wave height ( $H_s$ ), and infragravity wave height ( $H_i$ ) was calculated as follow:

$$H_s = 4 \sqrt{\int_{0.05}^{0.3} S df}$$



$$Hi = 4 \sqrt{\int_{0.001}^{0.05} S df}$$

where  $S$  is the power spectrum and  $f$  is wave frequency.

Similarly, the mean wave period and the infragravity wave period were calculated using the following equations:

$$Tms = \frac{\int_{0.05}^{0.3} S df}{\int_{0.05}^{0.3} S \cdot f df}$$

$$Tmi = \frac{\int_{0.001}^{0.05} S df}{\int_{0.001}^{0.05} S \cdot f df}$$

For each burst the wave energy flux ( $E$ ) was also calculated as:

$$E = \rho g S Cg$$

where  $\rho$  is the density of water;  $g$  is the acceleration due to gravity; and  $Cg$  is the wave group velocity which depends on the wave frequency and the depth.

### 3.2.2 Water levels

The water levels were corrected to reflect the elevation of the water table above Mean Sea Level (hereafter MSL).

### 3.2.3 Currents

Currents were averaged through the water column and are presented as Easterly/Northerly components.

### 3.2.4 Tide

A tide analysis was completed for the offshore water level using the T-Tide software (Pawlowicz et al. 2002). The form factor (Haigh et al. 2011) was calculated and compared with common ranges (Pugh, 2004).

## 4 Results

### 4.1 Waves

Waves were successfully recorded at all sites with little gaps at the shore, in mid reef and offshore. This provides 1.5 years of wave data across the reef. A short description of the result is presented below starting with the reef slope instrument.

#### 4.1.1 Reef slope

The mean wave height of short waves ( $T < 20s$ ) on the reef slope for all the record was 0.94m (Figure 4.1) with a mean wave period of 11s (Figure 4.2). For the duration of the record, 13 wave events had a significant wave height higher than 2m and the largest event was 3.22m. The 3 largest events all occurred between the 22 May 2013 and 30 of June 2013.

The infragravity wave heights recorded at the reef slope were much smaller than the short waves with a mean height of 0.08m. The largest infragravity wave height recorded was 0.62m and did not correspond to a large wave event (Figure 4.3). The mean wave period of the infragravity was 66s (Figure 4.4).

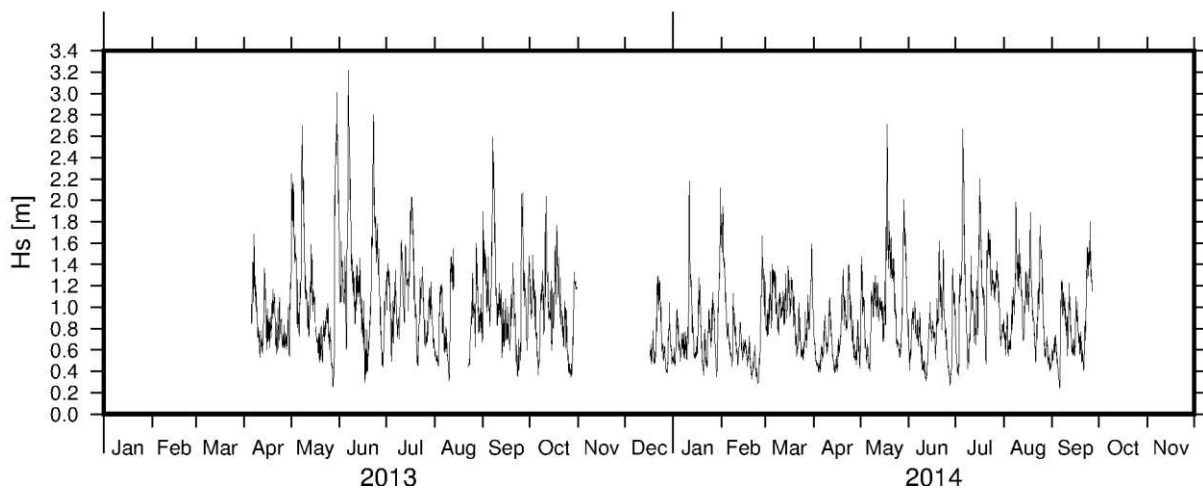


Figure 4.1: Significant wave height recorded on the reef slope

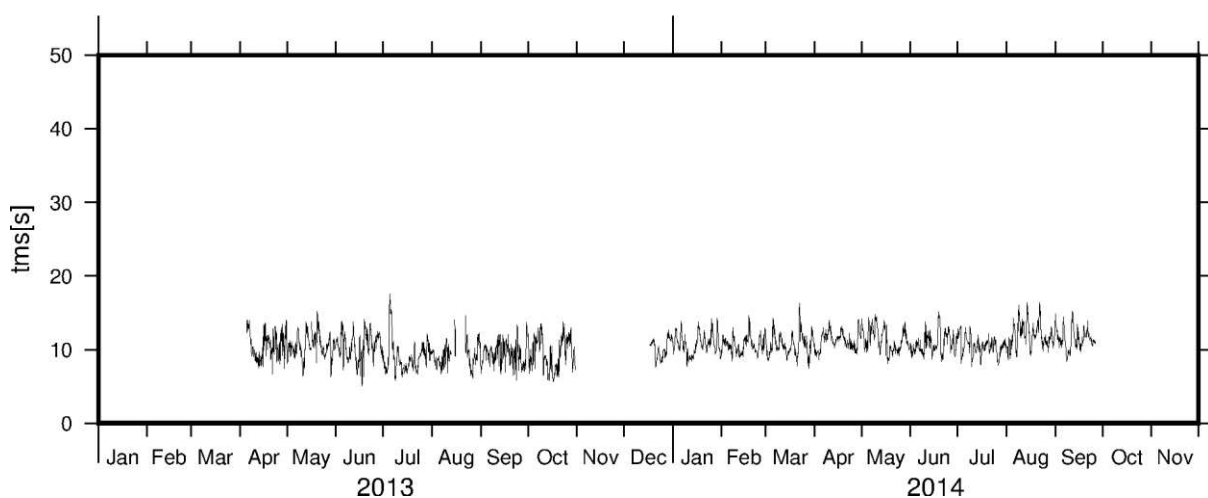


Figure 4.2 Mean wave period of short waves recorded on the reef slope

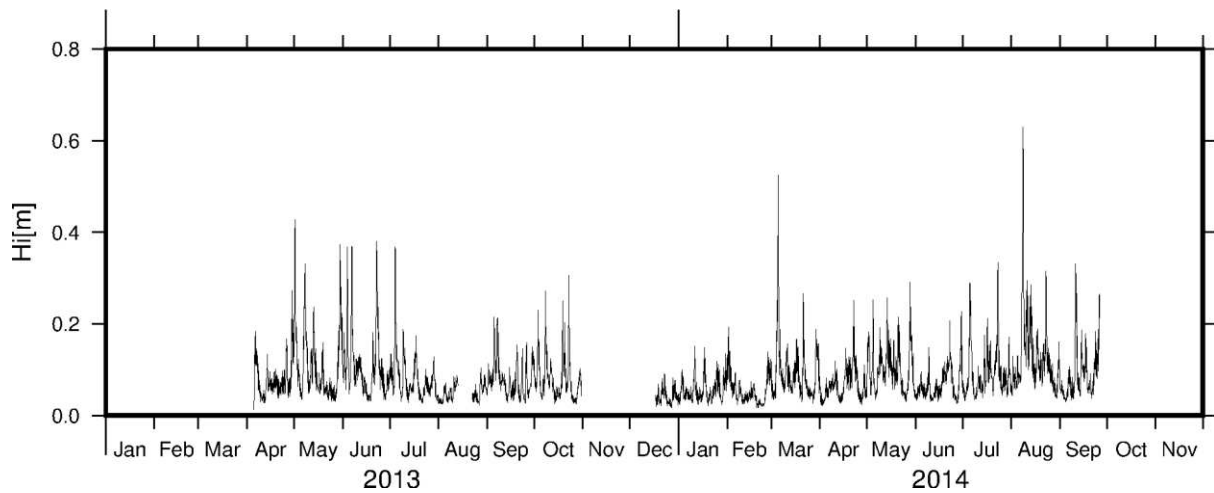


Figure 4.3 Infragravity wave height recorded on the reef slope

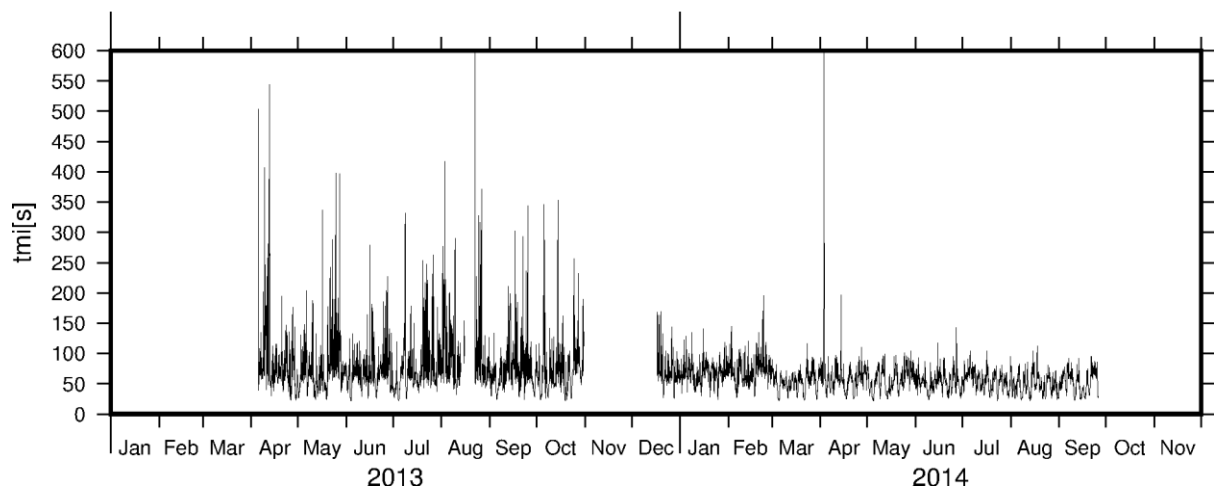


Figure 4.4 Mean wave period of infragravity waves recorded on the reef slope

#### 4.1.2 Reef crest

Waves on the reef crest were on average much smaller than on the reef slope with a mean significant wave height of 0.32m. The waves are also highly modulated by the tide. The largest significant wave height was measured at 1.07m on the 22 June 2013 (Figure 4.5). The mean wave period was similar than that of the reef slope site at 11s (Figure 4.6).

In contrast, the infragravity wave height is much larger at the reef crest than on the reef slope with a mean of 0.22m and exceeding 1.0m on 3 events in May and June 2013 (Figure 4.7). The mean period of the infragravity was 197s (Figure 4.8).

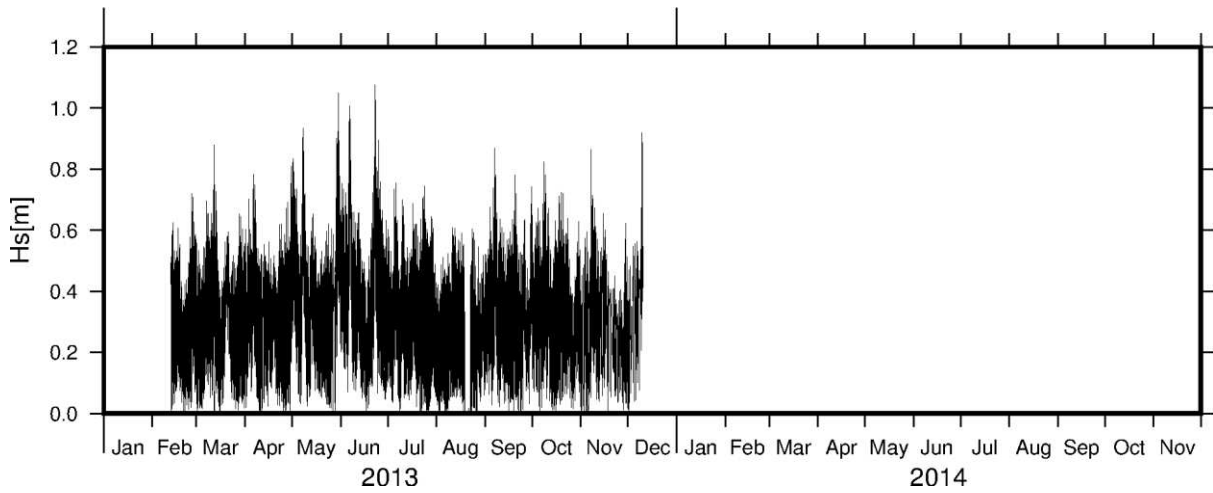


Figure 4.5 Significant wave height recorded on the reef crest

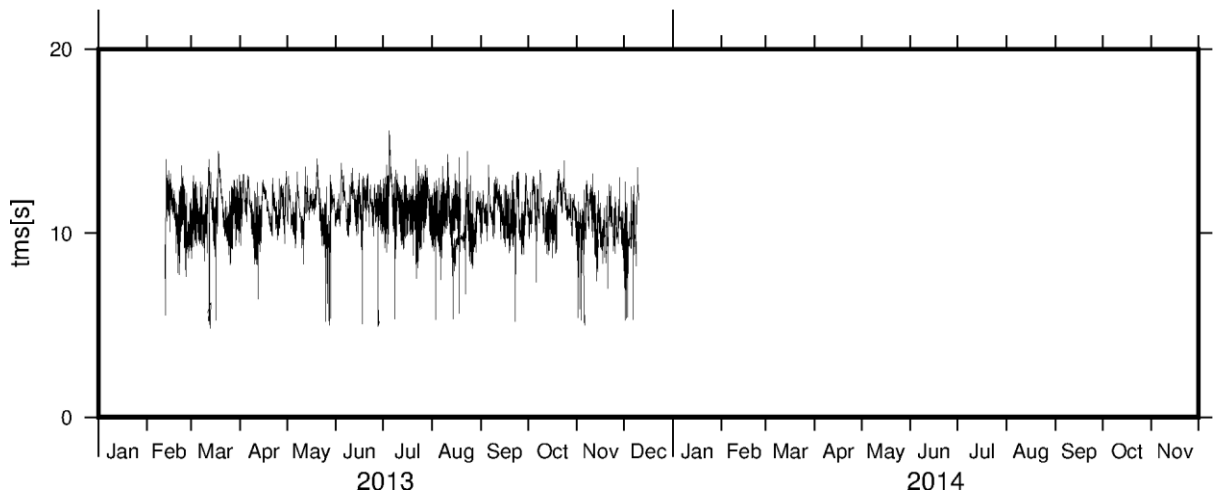


Figure 4.6 Mean wave period of short waves recorded on the reef slope

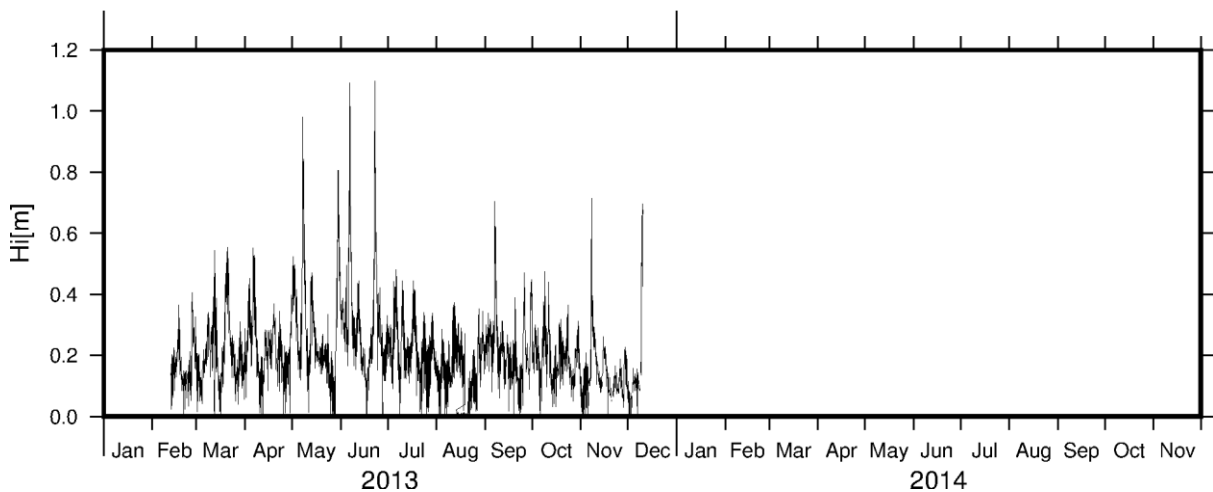


Figure 4.7 Infragravity wave height recorded on the reef crest

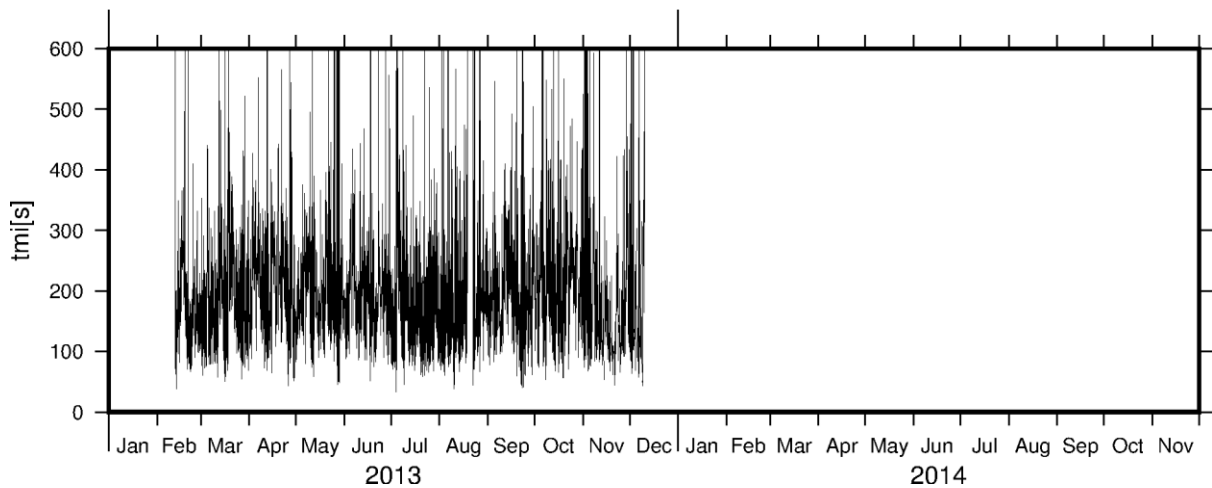


Figure 4.8 Mean wave period of infragravity waves recorded on the reef crest

#### 4.1.3 Mid-reef

Waves recorded, at the centre of the reef flat were much smaller than the waves recorded on the reef slope or the reef crest. The mean significant wave height at the mid-reef location was 0.03m with a mean period of 7s (Figure 4.9 and 4.10). Infragravity dominates the environment with a mean infragravity wave height of 0.06m with a mean period of 648s (Figure 4.11 and 4.12).

The largest infragravity wave height was recorded on 06 June 2013 at 0.67m. Both infragravity and short waves are highly modulated by the tide.

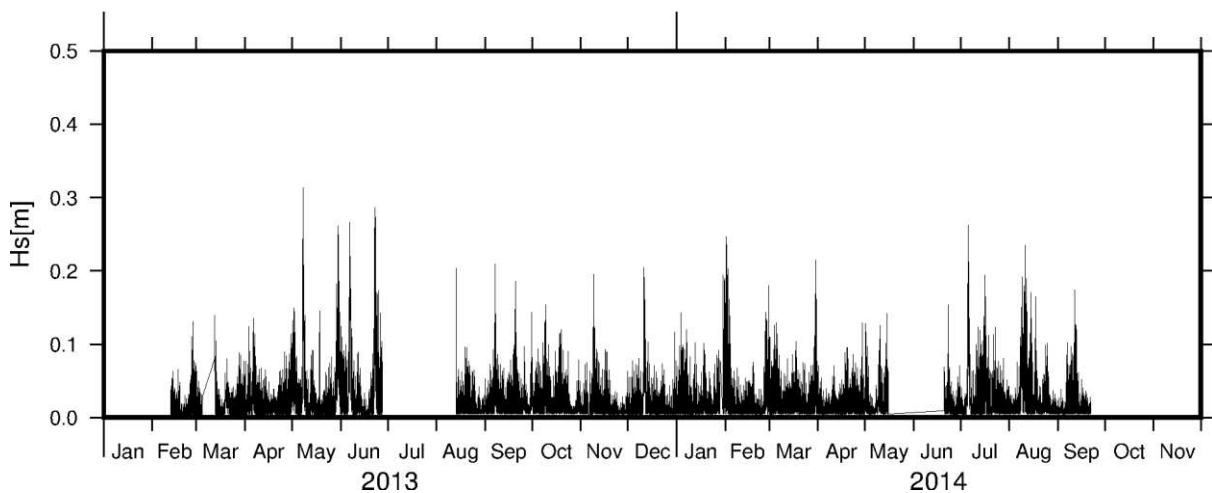


Figure 4.9 Significant wave height recorded mid-reef

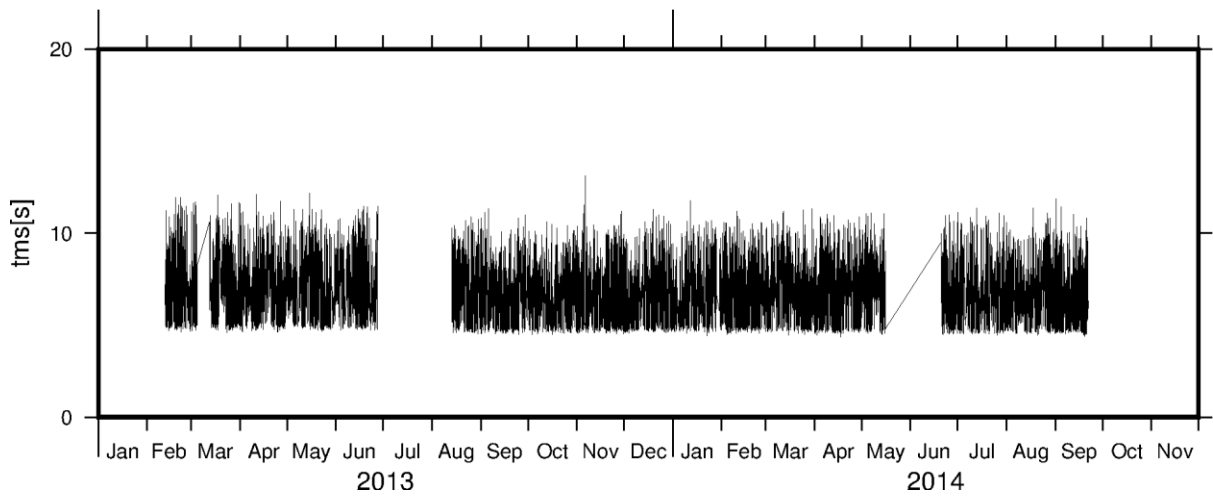


Figure 4.10 Mean wave period of short waves recorded mid-reef

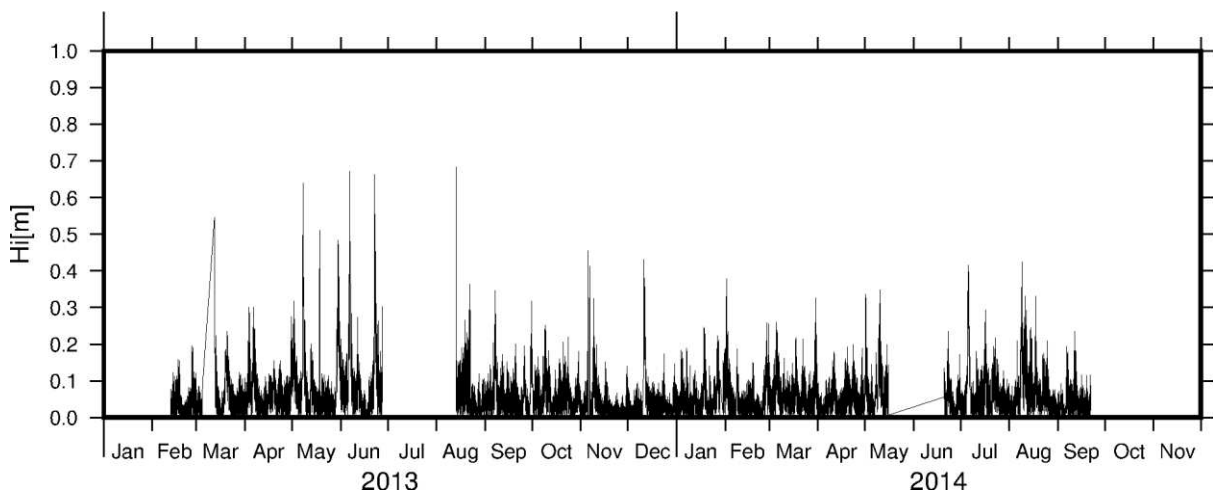


Figure 4.11 Infragravity wave height recorded mid-reef

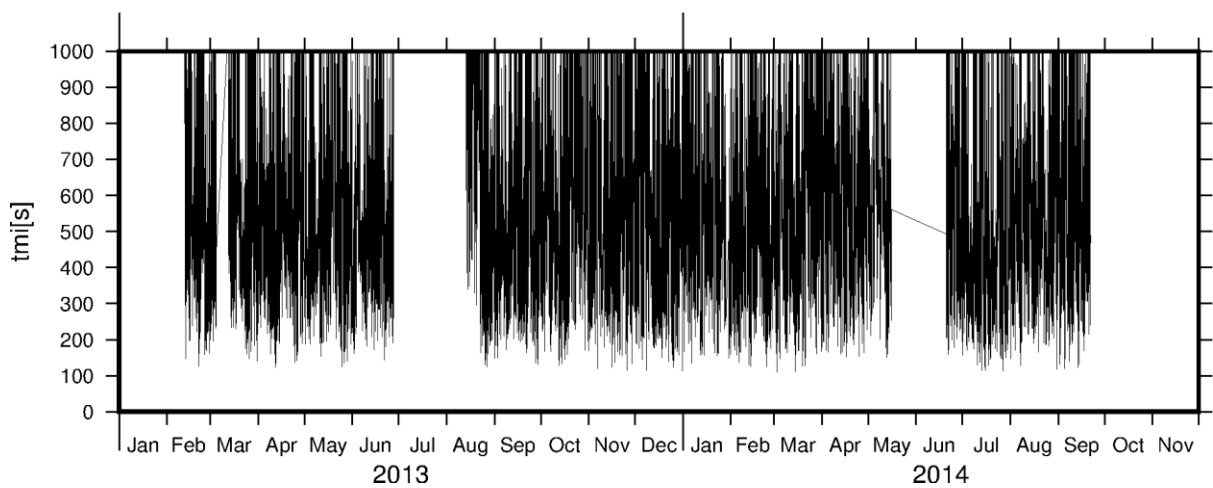


Figure 4.12 Mean infragravity wave period recorded mid-reef

#### 4.1.4 Shore

Waves recorded at the shore were similar to the waves recorded mid-reef. The mean significant wave height is 0.02m at 7s (Figure 4.13 and 4.14). Infragravity waves also dominate the shores with a mean infragravity wave height of 0.08m at 575s (Figure 4.15 and 4.16). The largest infragravity waves were recorded on the 8 May 2013 at 0.85m.

Similarly to the reef crest and the mid reef instrument, the shore location waves are modulated by the tide.

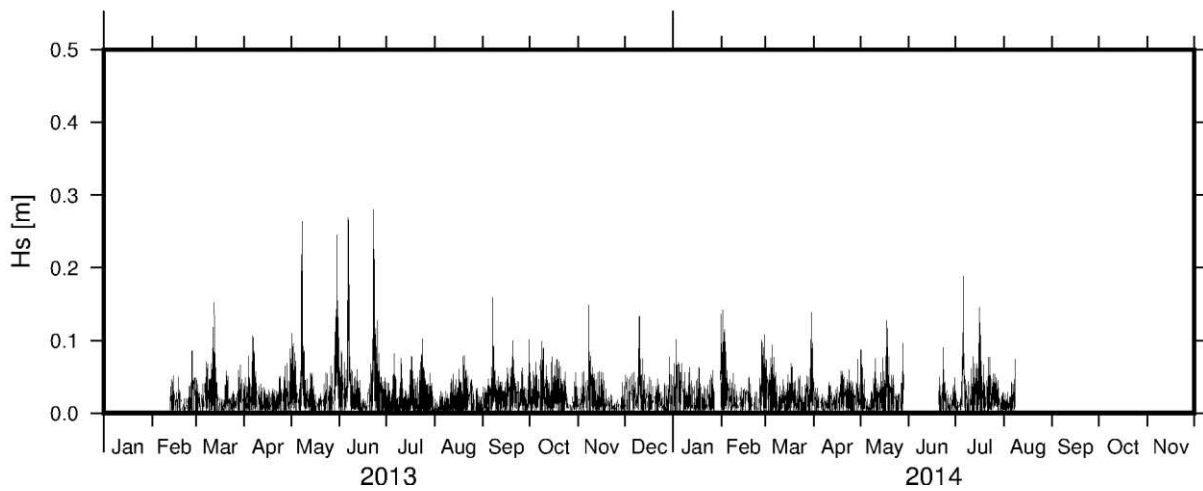


Figure 4.13 Significant wave height recorded on the shore

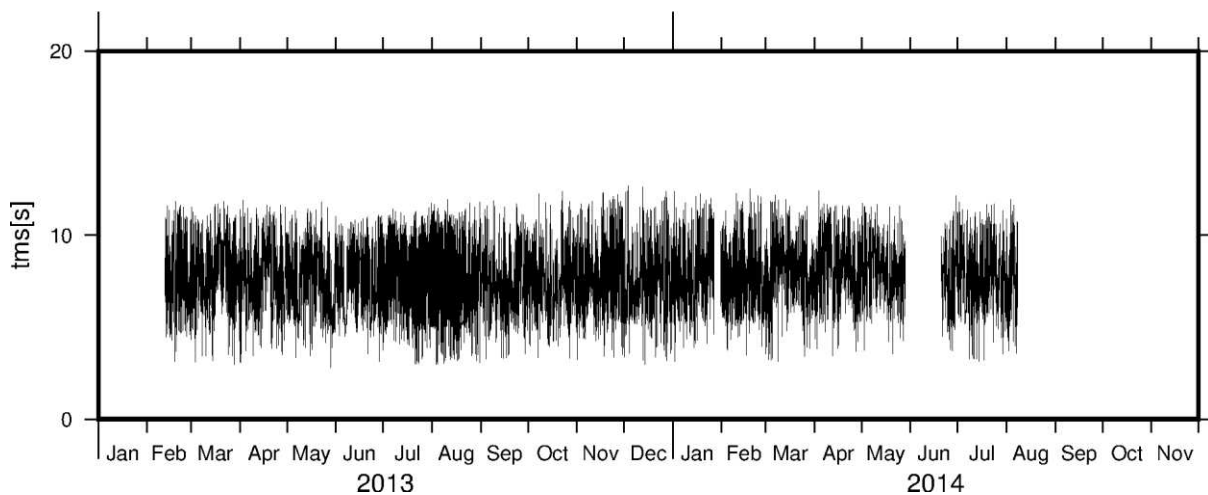


Figure 4.14 Mean wave period of short waves recorded on the shore

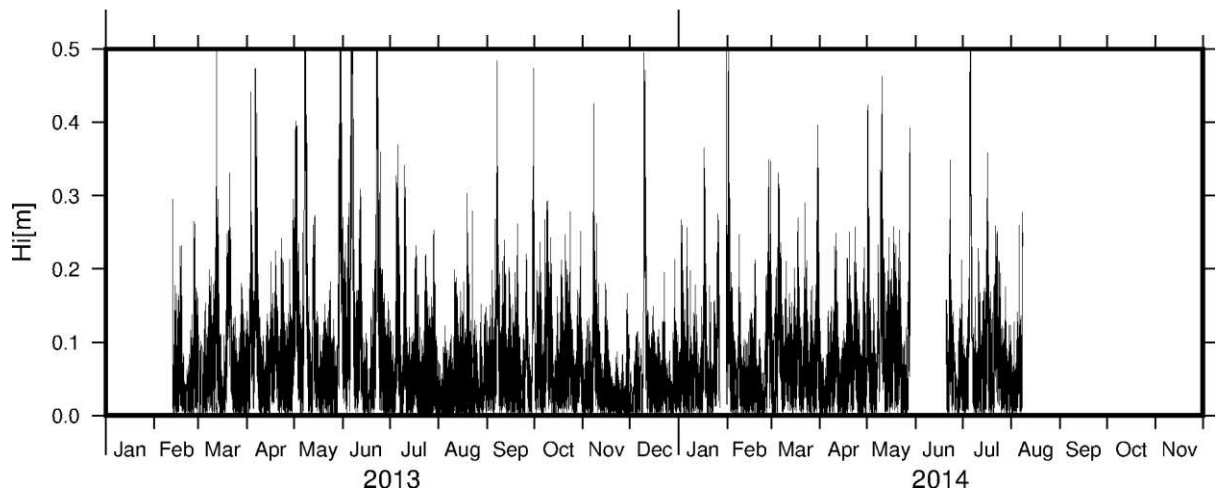


Figure 4.15 Infragravity wave height recorded at the shore

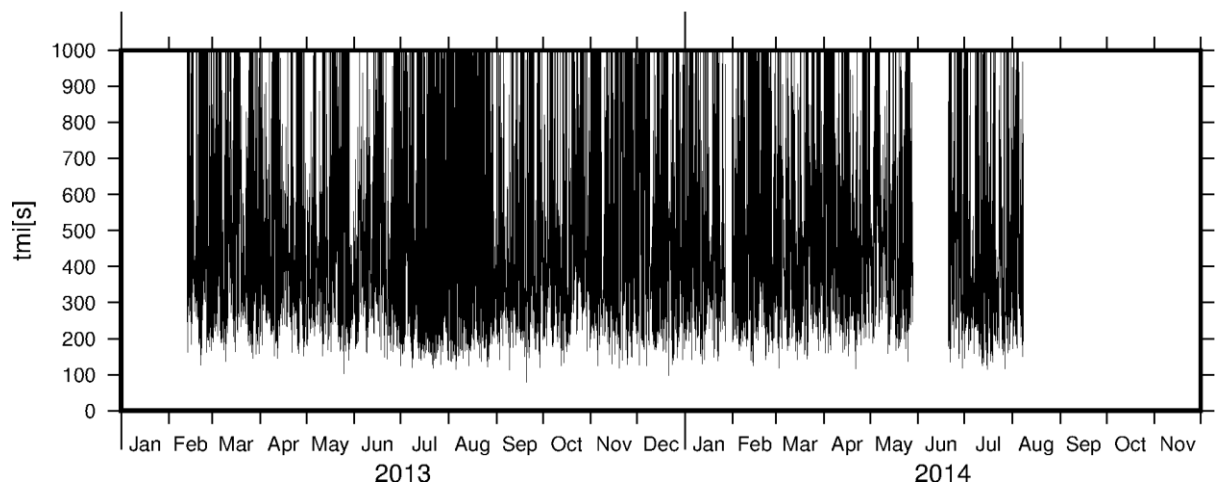


Figure 4.16 Mean infragravity wave period recorded at the shore

## 4.2 Water level

Water level inside reef systems is known to modulate waves.

### 4.2.1 Reef slope

Water level on the reef slope shows a classic semi-diurnal tide with spring and neap cycles. The largest water level was recorded on the 30 Jan 2014 at 1.02 m (above mean sea level). The lowest water level was recorded on the 1<sup>st</sup> Feb 2014 at -1.06m (Figure 4.17).



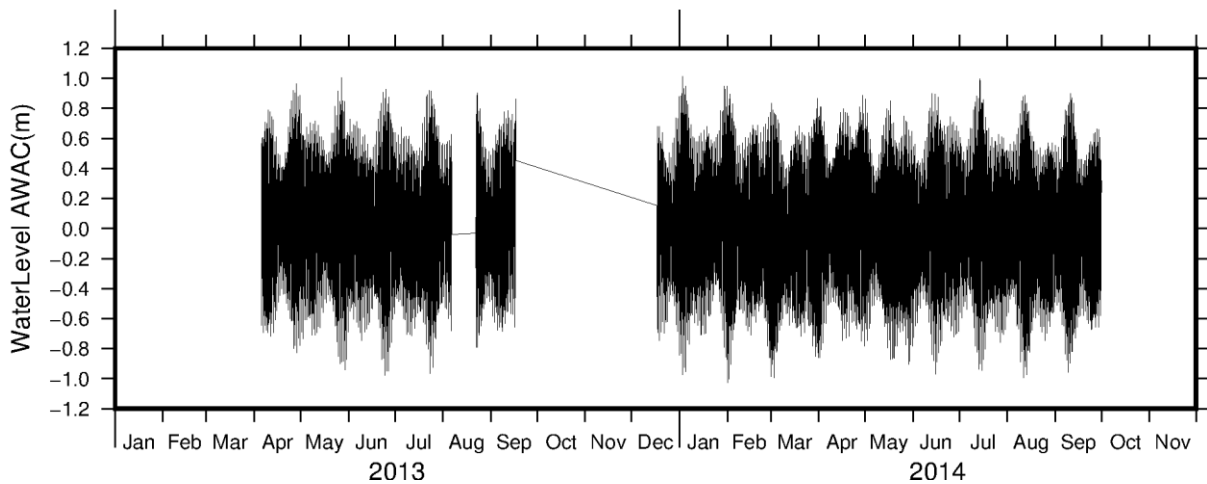


Figure 4.17 Water level measured on the reef slope. Note that zero is the mean water level for the deployment period

#### 4.2.2 Reef crest

Water level on the reef crest shows a very different signal than on the reef slope. The water level on the reef crest does not show low tide because the instrument dried out and also because the inside of the reef flat acts as a pool of water at low tide, hence the lowest recorded water level was -0.13m (relative to MSL). The mean water level for the record duration was 0.30m. The highest water level recorded on the reef crest was on the 22 June 2014 at 1.37m (Figure 4.18).

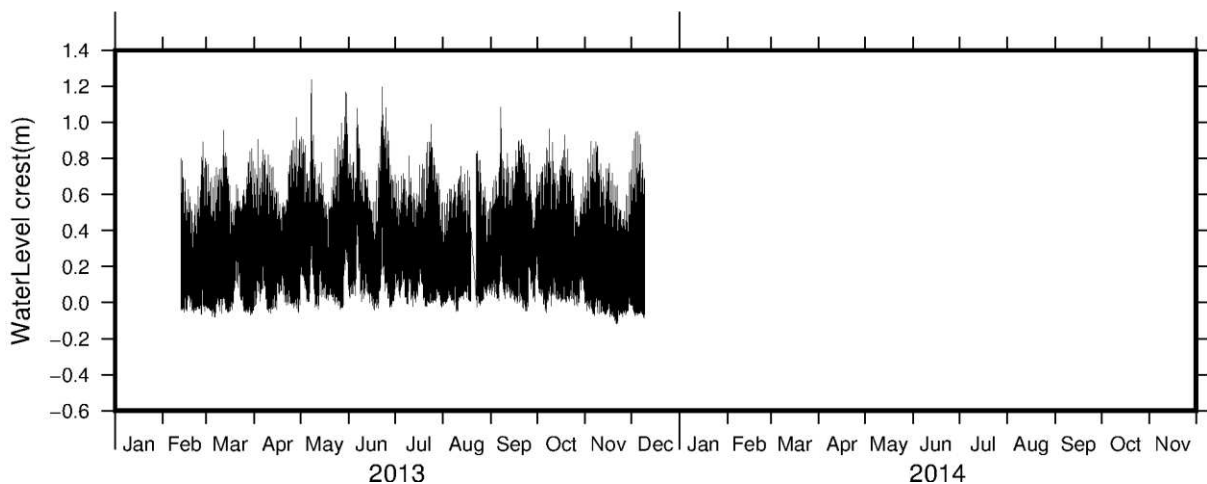


Figure 4.18 Water level measured on the reef crest. The water level was corrected so zero is the mean sea level

#### 4.2.3 Mid Reef

Similarly to the reef crest, the mid reef site does not show low tides. However the instrument remained submerged even at the lowest water level because of the water pools in the reef flat. The mean water level was 0.35m. The lowest water level was recorded on 31 December 2013 at -0.07m. The largest water level was recorded on the 6 June 2013 at 1.69m (Figure 4.19).

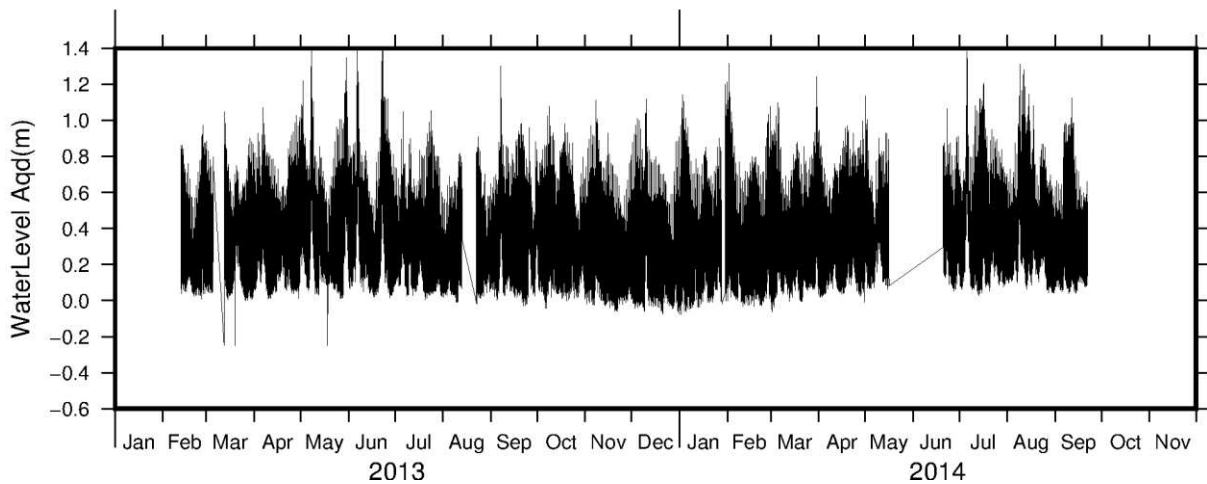


Figure 4.19 Water level measured on the mid reef. The water level was corrected so zero is the mean sea level

#### 4.2.4 Shore Water level

At the shore the water levels are very similar to the mid reef location. The mean water level was 0.34m. The lowest water level was recorded on 02 March 2014 at -0.06m. The highest water level was recorded on 8 May 2013 at 1.70m (Figure 4.20).

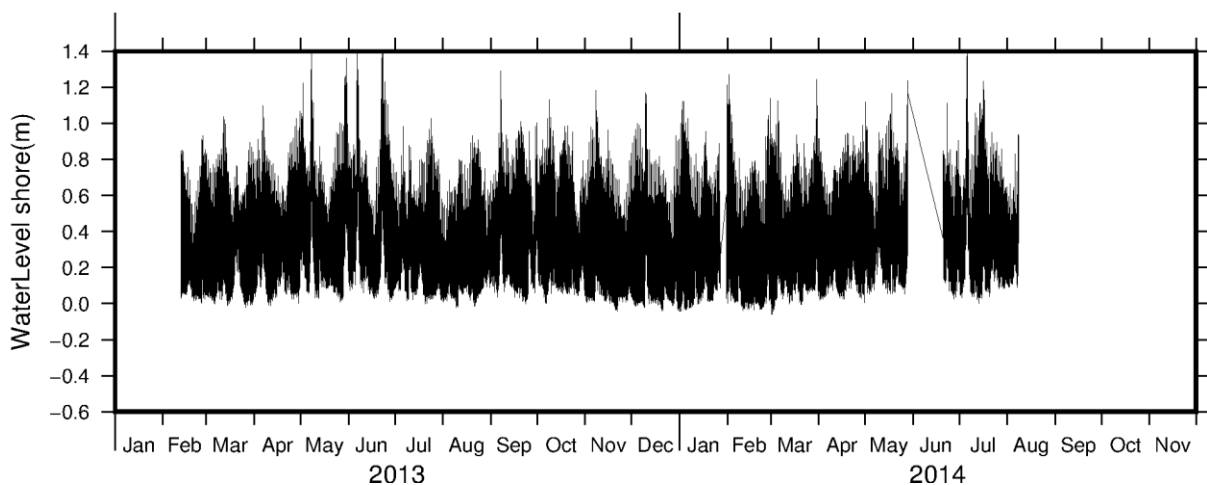


Figure 4.20 Water level measured on the shore. The water level was corrected so zero is the mean sea level

### 4.3 Temperature

Temperatures were also recorded at each of the locations.

#### 4.3.1 Reef slope

The mean water temperature on the reef slope at 20m depth was 27.5°C. The maximum temperature was recorded on 21 February 2014 at 30.8°C. The minimum temperature was recorded on 27 August 2014 at 24.8°C. Although the temperature signal is not clearly modulated by the tide; there are evidence of sharp temperature variation of 1–3°C within a tidal cycle between December 2013 and March 2014 which may be related to the activity of internal waves forming along a well-defined thermocline (Figure 4.21).

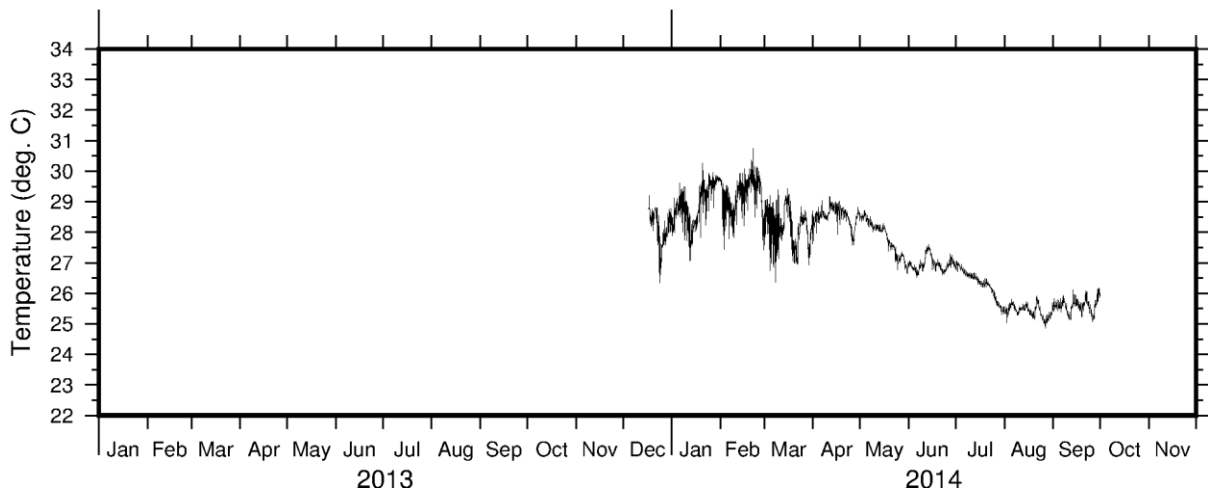


Figure 4.21 Water temperature at 20m depth on the reef slope in Maui Bay

### 4.3.2 Reef crest

On the reef crest, the temperature sensor was temporarily emerged or in small water pools making the temperature variable. The mean water temperature on the reef crest was 27.2°C. The maximum temperature was recorded on 16 March 2013 at 36.0°C. The minimum temperature was recorded on 27 August 2013 at 20.1°C (Figure 4.22).

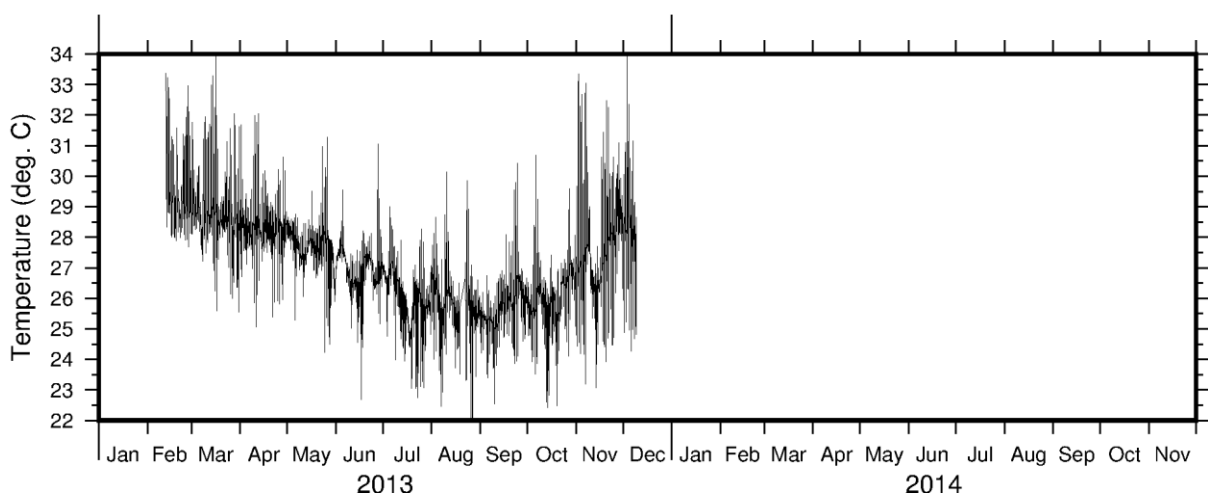


Figure 4.22 Sensor temperature on the reef crest in Maui Bay. Note at low tide the instrument was emerged and temperature during that time may be representative of water pooling near the instrument.

### 4.3.3 Mid Reef

At the mid reef, the water temperature is affected by the tide and the swell that bring in cooler offshore water. The mean water temperature was 27.5°C. The maximum temperature was recorded on 13 February 2014 at 34.1°C. The minimum temperature was recorded on 27 July 2014 at 21.8°C (Figure 4.23).

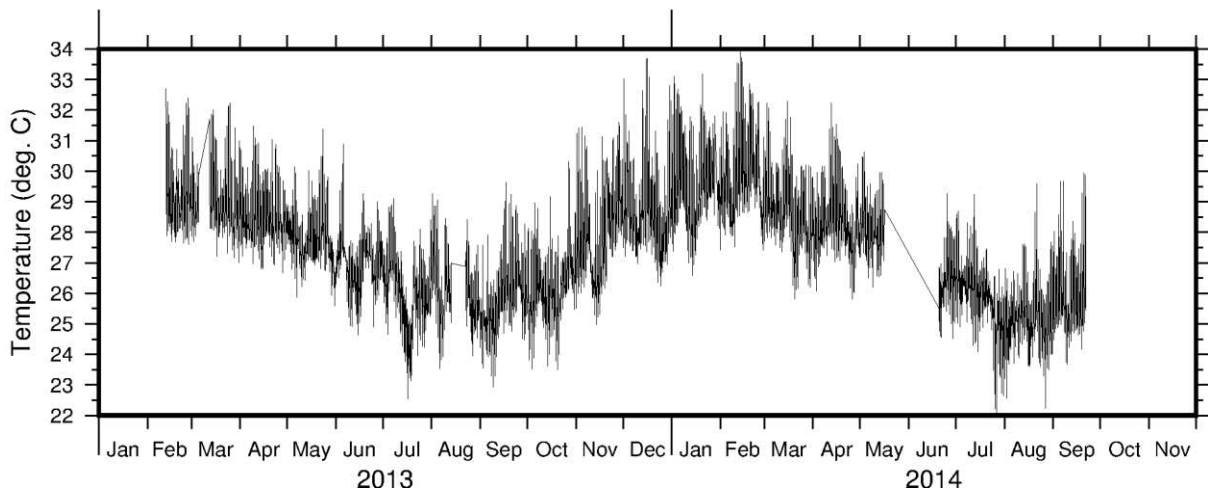


Figure 4.23 Water temperature at mid reef in Maui Bay

#### 4.3.4 Shore

Temperature variations due to tide and swell (or lack of) are even more pronounced at the shore. Here the cooler waters suggest a higher influence of wind and air temperature. The mean water temperature was 27.8°C. The maximum temperature was recorded on 20 January 2014 at 34.3°C. The minimum temperature was recorded on 27 July 2014 at 20.9°C (Figure 4.24).

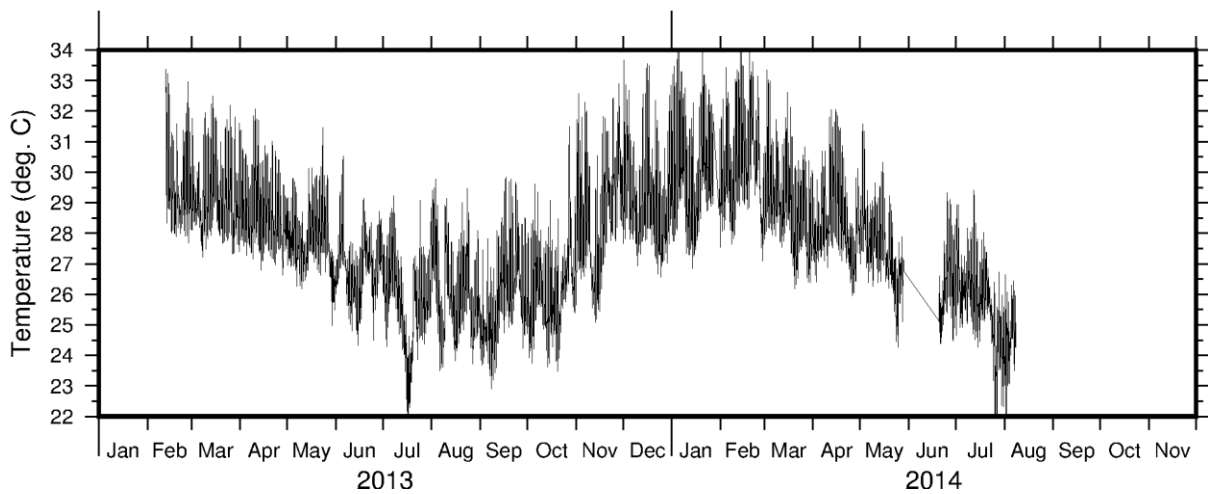


Figure 4.24 Water temperature at the shore in Maui Bay.

#### 4.4 Tides

Tides are evidently an important oceanographic process in Maui Bay. However the water levels on the reef flat are mostly controlled by waves which are modulated by the tide. To better understand the role of the tide a tidal analysis of the water level measured on the reef crest was conducted.

Tidal analysis provided the amplitude and phase of the principal constituent of the tide (Table 4.1). The tide form factor was calculated as 0.24 which correspond to a semidiurnal form.

Table 4.1 Amplitude of tidal constituents in Maui Bay extracted from offshore water levels

Constituent	M2	S2	N2	K1	K2	O1	P1	SSA
Amplitude (m)	0.5727	0.1069	0.1310	0.1104	0.0253	0.0529	0.0324	0.0135

#### 4.4.1 Exceedance Curve

The Mean High Water Perigean Spring high tide often referred to as “King tides” is the amplitude of the M2, S2 and N2 tidal harmonics, this tidal level (0.8106m) (Table 4.2) is exceeded by 8% of high tides. The mean high water spring (Spring high tides) is the combined amplitude of the M2 and S2 tidal harmonics (0.6796m), here exceeded by 19% of high tides. The Mean high Water is the mean elevation of all high tide (0.5835) and the Mean High Water neap is the difference in amplitude of the M2 and S2 tidal harmonics level of the tide (0.4658) exceeded by 90% of high tides (Figure 4.25).

Table 4.1 Common tidal elevation for Maui Bay offshore waters

	Mean High Water Perigean Spring (MHWPS)	Mean High Water Spring (MHWS)	Mean High Water (MHW)	Mean High Water Neap (MHWN)
Values (m above mean sea level)	0.8106	0.6796	0.5835	0.4658

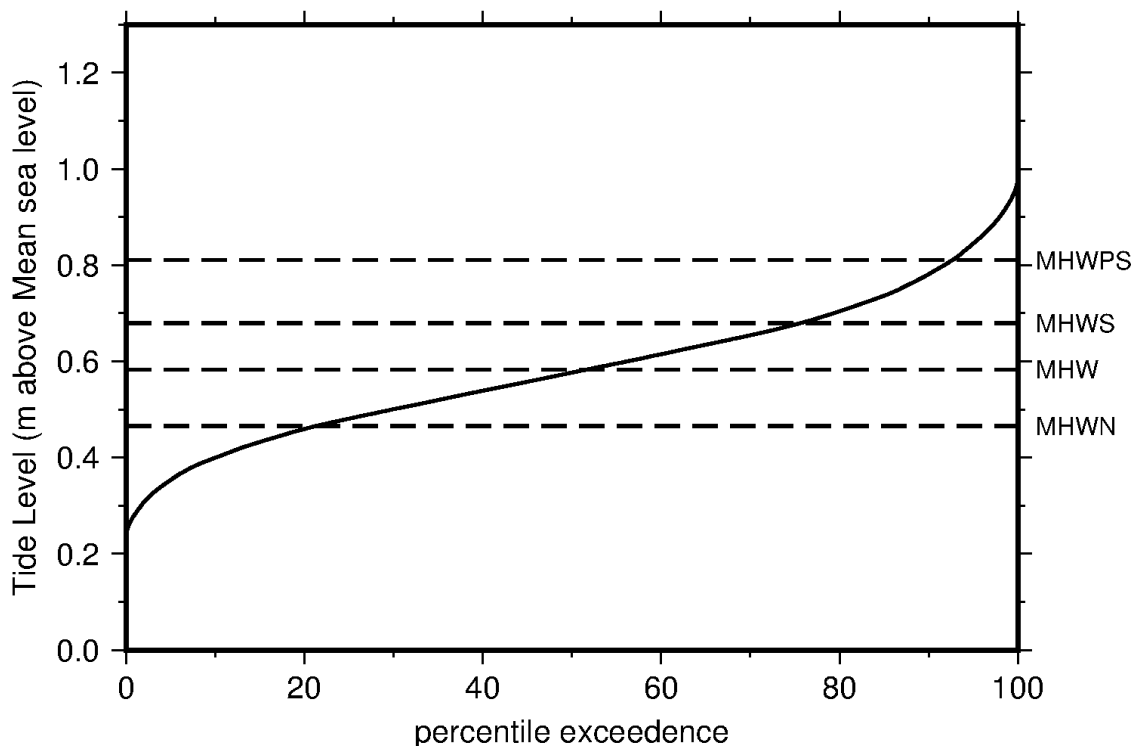


Figure 4.25 Tidal level percentile exceedance curve

## 4.5 Currents

Currents were only measured offshore and at the mid reef location. On the offshore side the depth averaged currents are mostly alongshore modulated by both wind and tides (Figure 4.26). On the mid reef flat, the depth averaged currents are modulated by infragravity waves and oriented toward the shore (Figure 4.27).

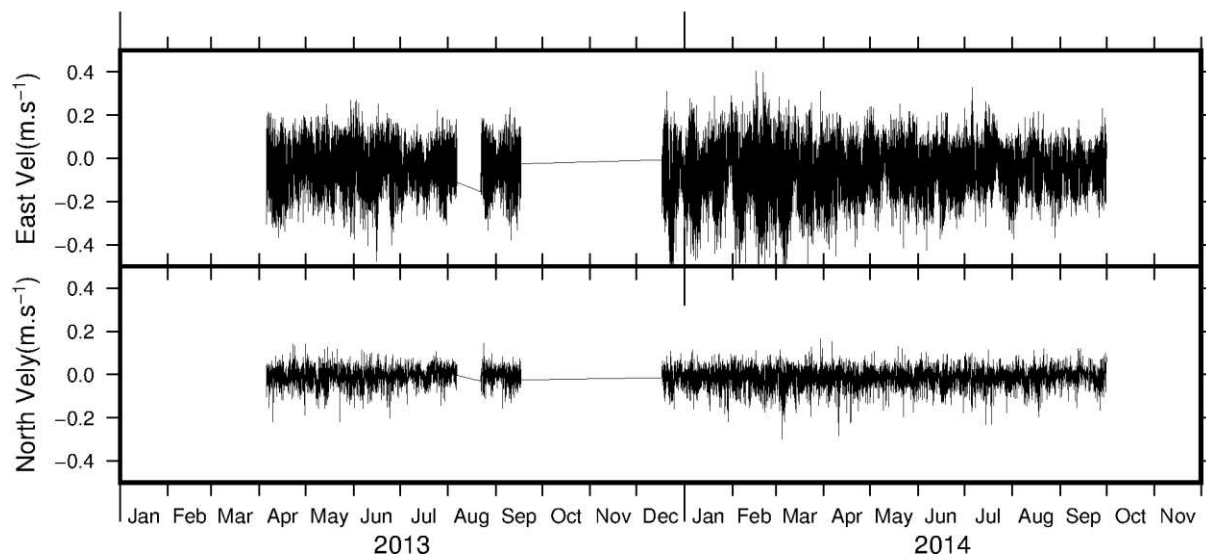


Figure 4.26 Depth averaged Cartesian Currents measure on the reef slope

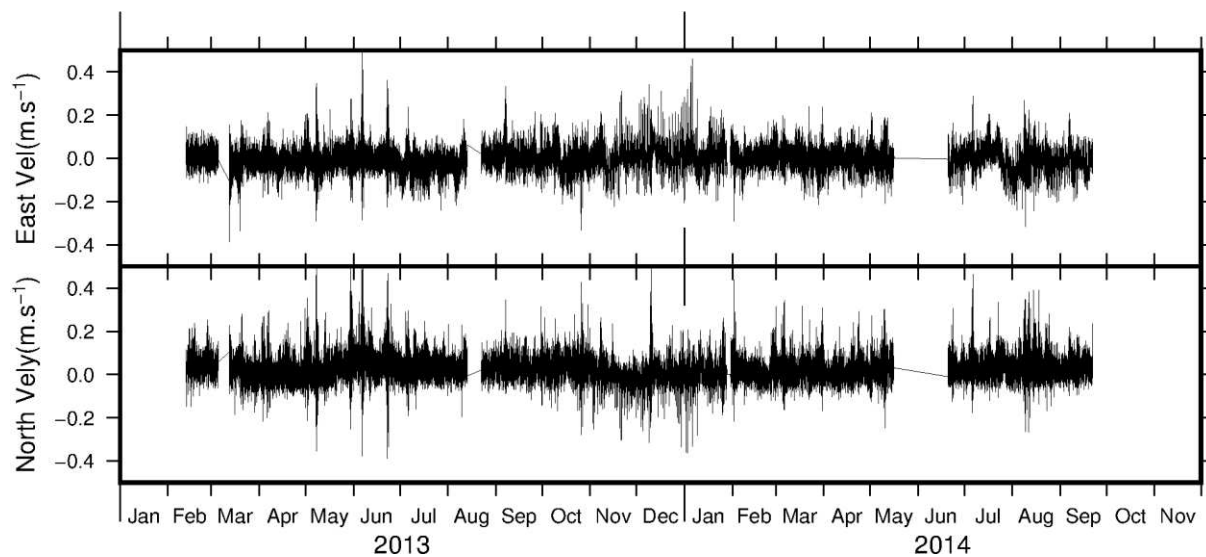


Figure 4.27 Depth averaged Cartesian Currents measure mid reef

## 5 Discussion

The large amount of data collected in Maui Bay has uncovered some interesting oceanographic aspect of Fringing reef hydrodynamics. Here we discuss further how the reef morphology is creating an enclosed basin limiting the drainage of water and how the relatively shallow water is a suitable environment for the generation of large infragravity waves.

## 5.1 Tide and wave setup in the reef flat

In Maui Bay, the water levels measured on the reef slope (i.e. offshore) shows a typical semidiurnal tide. During calm weather, when waves are small, the high tide at all recorded locations are identical. But low tides on the reef crest and the reef flat are quite different.

The reef crest elevation approximately corresponds to -0.1m MSL and when the water level offshore reaches below 0.4m the water from the reef flat flow offshore over the reef crest as a turbulent, critical to supercritical flow. As the water depth lowers on the reef flat, the velocity of the flow and hence the speed of the drainage slows down (Figure 5.1).

A similar process occurs on the algal ridges on either sides of the reef flat. When the water level reaches below 0.4m MSL, the water flow over the ridges become supercritical and the water drains out of the reef flat more slowly until the tide comes back to approx. 0.05m MSL. This slowing of the drainage of the water inside the reef system is common on perched tidal pools and a sign of a recent drop in relative water level either from an uplifting of the land or from the hydroisostasy rebound from 1.5—5Ky BP (Grossman et al. 1998).

Carbon dating of shells collected on the beachrock in Maui Bay was dated at 3000 years BP. These dates correspond well with the sea level high stand due to hydroisostatic rebound affecting the whole Pacific.

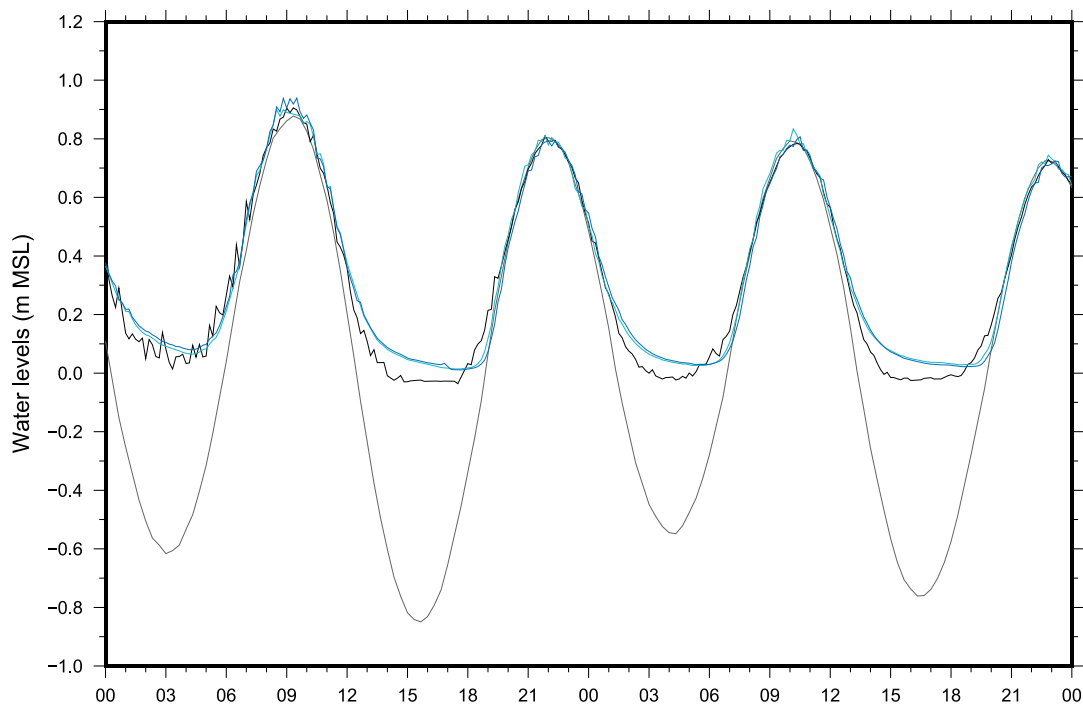


Figure 5.1 Water levels measured between the 29 and 30 June 2013. Grey water level on the reef slope

Figure 5.2

## 5.2 Infragravity waves

During large waves the wave set up inside the reef flat can be larger than the tide. In May and June 2013, 4 wave events had significant wave height of 3m, and at the peak of these events the wave set up on the reef flat was nearly 1m (Figure 5.2). During these events waves continued to push water inside the reef system even at low tide. The large infragravity waves were observed inside the reef system sometimes exceeding 1m height, these are locally known as Loka waves. The Loka waves were found to be well correlated with wave group offshore although delayed by a slow travelling time (Figure 5.3). This suggests that the Loka waves are the result of wave groups piling water on the shallow reef flat that later propagates as an infragravity wave. While propagating on the reef flat the Loka waves were found to dissipate from bottom friction and breaking of the hydraulic jump bores. Loka waves were found to be highly asymmetrical and hydraulic jump were also observed forming on the leading wave faces forming solitons on the crest of the waves (Figure 5.4) these bores have been observed to break, dissipating the infragravity waves further.

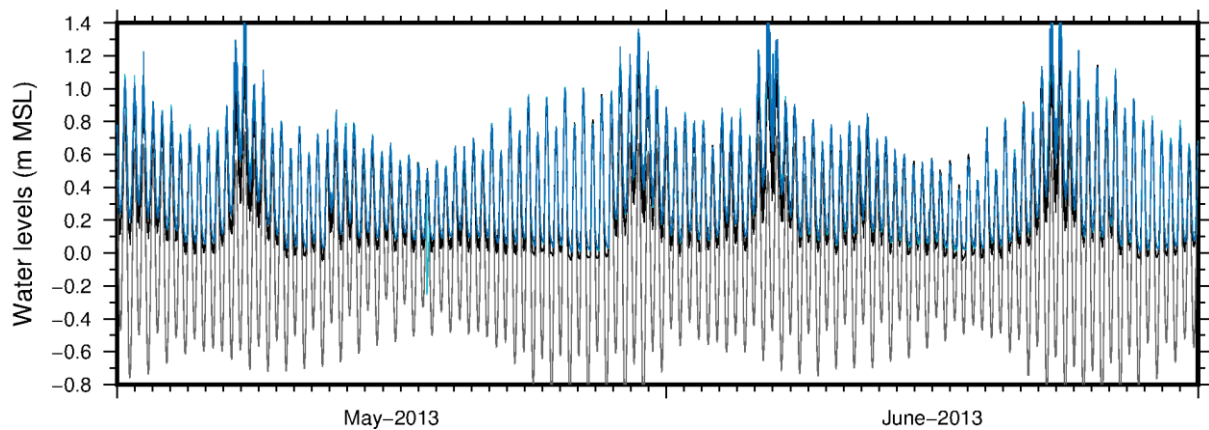


Figure 5.2 Water level recorded offshore (grey line), on the reef crest (black line) and the shore (blue line).

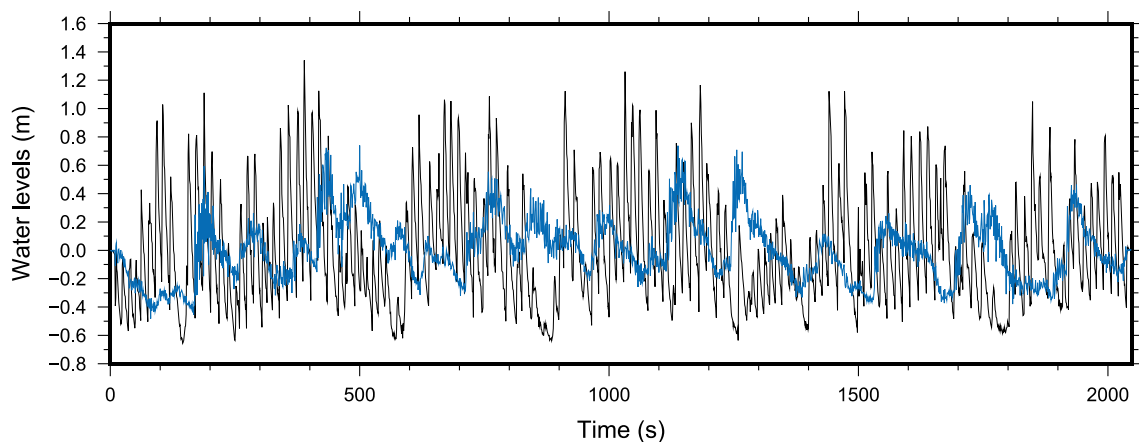


Figure 5.3 Water level recorded at 1Hz on the reef crest (black line) and the shore (blue line)



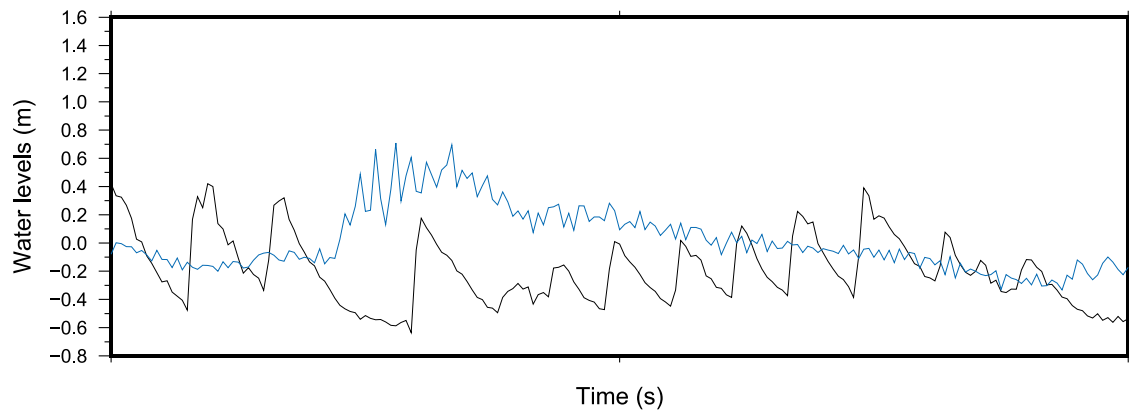


Figure 5.4 Infragravity waves observed at the shore (blue line). Each tick on the x axis corresponds to 100 seconds.

Infragravity waves were also observed and dominating the hydrodynamics of the reef flat during fair weather condition. The infragravity wave asymmetries suggest they are responsible for a shoreward flux of sediment on the reef flat. Infragravity waves are not only a major contributor to coastal inundation but also control the sediment transport on the beaches even in fair weather condition.

## 6 Conclusion

Observation of waves and water level shows that long period infragravity wave dominate the dynamics of the fringing reef system in Maui Bay. The dataset presented in this report has been briefly analysed here and can yield far more results pending deeper analysis and numerical modelling. The Maui Bay offshore site has been selected for long term wave monitoring for Fiji and data collection will continue indefinitely.

## 7 Data download and Citation

The processed data presented in this report may be downloaded on the PacGeo web portal

Wave data offshore

<http://www.pacgeo.org/documents/2928>

Wave data Reef crest

<http://www.pacgeo.org/documents/2927>

Wave data mid reef

<http://www.pacgeo.org/documents/2926>

Wave data shore

<http://www.pacgeo.org/documents/2925>

Water levels and temperature offshore

<http://www.pacgeo.org/documents/2933>

Water level and Temperature crest

<http://www.pacgeo.org/documents/2930>

Water level and Temperature mid-reef

<http://www.pacgeo.org/documents/2931>

Water level and Temperature shore

<http://www.pacgeo.org/documents/2932>

The raw data can be freely obtained upon request to the authors.

When using the data for publication, please cite this report:

Bosserelle C., Lal D., Reddy S., Movono M., Begg Z., Kumar S., Krüger J. Maui Bay (Fiji), oceanographic data collection, WACOP project, SPC technical report SPC00036, 2016

## 8 Reference

Bosserelle, C., Kruger, J., Movono, M., Reddy, S., (2015) Wave inundation on the coral coast of Fiji, Australasian Coasts & Ports Conference 2015: 22nd Australasian Coastal and Ocean Engineering Conference and the 15th Australasian Port and Harbour Conference

Haigh, I. D., Eliot, M., & Pattiaratchi, C. (2011). Global influences of the 18.61 year nodal cycle and 8.85 year cycle of lunar perigee on high tidal levels. *Journal of Geophysical Research*, 116(C6), C06025. doi:10.1029/2010JC006645

Grossman, E. E., Fletcher, C. H., & Richmond, I. I. B. M. (1998). The Holocene sea-level highstand in the equatorial Pacific : analysis of the insular paleosea-level database, 309–327.

Pawlowicz, R., Beardsley, B., and Lentz, S. (2002), Classical tidal harmonic analysis including error estimates in MATLAB using T\_TIDE, *Computers and Geosciences* 28, 929-937.

Pugh, D. T. (2004), *Changing Sea Levels: Effects of Tides, Weather and Climate*, 280 pp., Cambridge Univ. Press, Cambridge, U. K.









CONTACT DETAILS  
Pacific Community

SPC Headquarters  
BP D5,  
98848 Noumea Cedex,  
New Caledonia  
Telephone: +687 26 20 00  
Fax: +687 26 38 18

SPC Suva Regional Office  
Private Mail Bag,  
Suva,  
Fiji,  
Telephone: +679 337 0733  
Fax: +679 337 0021

SPC Pohnpei Regional Office  
PO Box Q,  
Kolonias, Pohnpei, 96941 FM,  
Federated States of Micronesia  
Telephone: +691 3207 523  
Fax: +691 3202 725

SPC Solomon Islands  
Country Office  
PO Box 1468  
Honiara, Solomon Islands  
Telephone: +677 25543 /  
+677 25574  
Fax: +677 25547

Email: [spc@spc.int](mailto:spc@spc.int)  
Website: [www.spc.int](http://www.spc.int)